

Title No. 114-S99

Fatigue Resistance of Steel Fiber-Reinforced Concrete Deep Beams

by Benard Isojeh, Maria El-Zeghayar, and Frank J. Vecchio

An investigation of the fatigue resistance of small-scale steel fiber-reinforced concrete deep beams with steel fiber-volume ratios of 0, 0.75, and 1.5% is reported. The behavior of steel fibers in enhancing the fatigue life of deep beams and reducing the congestion of reinforcement in concrete is studied, and the possibility of obtaining optimized structural sections that are cost-effective using steel fiber-reinforced concrete is verified. Evolutions and inclinations of average principal strains and bond strength between concrete and steel reinforcing bars within the shear spans were also observed. The use of steel fibers, especially with a volume ratio of 1.5%, was observed to reduce the progressive strain values in concrete and steel reinforcing bars, hence resulting in enhanced fatigue life. No significant evolution profile was observed for the inclination of the principal directions, while the use of adequate anchorage preserved the bond strength between concrete and steel reinforcement. In all specimens, fracture of the longitudinal reinforcing bars occurred at failure, and fiber pullout was more prevalent than fiber breakage.

Keywords: deep beam; fatigue; steel fiber; strain evolution; strength; wind turbine foundations.

INTRODUCTION

In practice, some elements of fatigue-sensitive structures such as wind turbine foundations, offshore structures, transfer girders, and pile caps are generally designed as deep beams. Due to the dynamic nature of loading while in service, these structures are susceptible to fatigue failure resulting from reinforcement fracture, crushing of concrete struts coupled with irreversible compressive strain accumulation, or excessive opening of concrete cracks. As such, it is expedient that designs guard against the occurrence of such failure modes during the service life of the structure.¹⁻³

In the literature, the fatigue failure resistance of deep beams has been shown to be enhanced using increased amounts of vertical or longitudinal reinforcement. The use of horizontal or inclined web reinforcement has also been reported to enhance the fatigue life of deep beams.^{1,2} Although the provision of more reinforcing bars and the use of inclined reinforcement have been shown to enhance fatigue resistance performance, the congestion of reinforcement⁴ during construction has prompted further investigation of other possible means. Additionally, the need for optimized designs involving cost-effective and reduced sizes of fatigue-prone structures necessitates the consideration of other enhanced concrete composites.^{5,6}

Steel fiber-reinforced concrete exhibits improved properties such as increased toughness, ductility, and crack-bridging attributes that result in the increase of the load resistance capacity when compared to conventional reinforced concrete. The enhancing performance of steel fibers, especially after

cracking of concrete, has been attributed to the ability of the fibers to delay crack growth by bridging the crack surfaces.⁷⁻⁹

At the materials level, flexural fatigue tests conducted on steel fiber-reinforced concrete prisms by Chenkui and Guofan,⁵ Ramakrishnan et al.,¹⁰ Nanni,¹¹ Chang and Chai,¹² and Naaman and Hammoud¹³ all indicate enhanced fatigue life and reduced progressive deformation when compared with plain concrete prisms. It has also been reported that steel fiber-reinforced concrete beams subjected to fatigue stresses below the observed endurance limit exhibited increases in strength when subsequently subjected to monotonic loading.

In steel fiber-reinforced concrete beams also containing conventional longitudinal reinforcement, the influence of steel fiber crack-bridging reduces the induced stresses in the longitudinal reinforcing bars; hence, the number of cycles at which fracture will occur in the steel reinforcing bars is increased compared to conventional reinforced concrete without steel fibers.¹⁰ Experimental investigations on the fatigue behavior of steel fiber-reinforced concrete beams are scarce and, prior to the investigation reported in this paper, no fatigue tests conducted on steel fiber-reinforced concrete beams with shear span to effective depth ratios less than 2.5 had been reported. However, tests conducted by Kormeling et al.¹⁴ on beams governed by flexure showed the enhancing effects of steel fibers on fatigue life, progressive deflection, and crack width growth.

The significant influence of steel fibers in reinforced concrete beams under fatigue loading has been reported by Kwak et al.¹⁵ through tests conducted on steel fiber-reinforced concrete beams with shear span to effective depth ratio of 2.5. The fatigue failure mechanism of steel fibers using different volume ratios was observed to be a result of fiber fracture rather than pullout.

Parvez and Foster^{16,17} investigated the influence of steel fibers on the fatigue behavior of small-scale and large-scale reinforced concrete beams governed by flexure. The final failure mechanism in all beams was by fracture of the longitudinal reinforcement. Generally, it was reported that steel reinforcing bar fracture propagation governed the fatigue life of under-reinforced beams. Further, the fatigue life of beams with steel fibers was enhanced and the measured deformations and stresses were observed to decrease as the volume ratio increased from 0% to 0.8%.

ACI Structural Journal, V. 114, No. 5, September-October 2017.

MS No. S-2016-339.R1, doi: 10.14359/51700792, received September 30, 2016, and reviewed under Institute publication policies. Copyright © 2017, American Concrete Institute. All rights reserved, including the making of copies unless permission is obtained from the copyright proprietors. Pertinent discussion including author's closure, if any, will be published ten months from this journal's date if the discussion is received within four months of the paper's print publication.

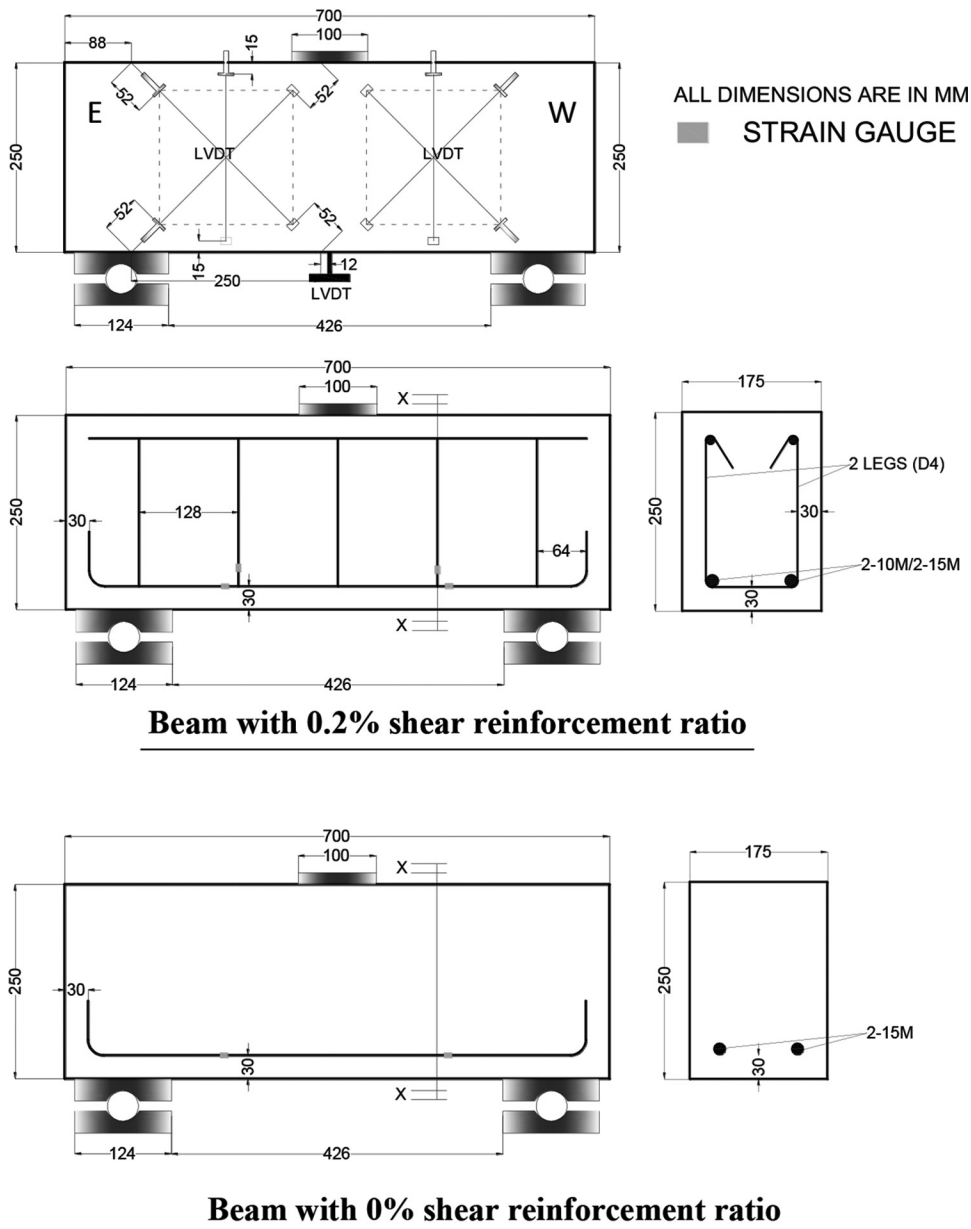


Fig. 1—Details of deep beam specimen.

Although Parvez and Foster¹⁷ reported that the reduction in steel reinforcing bars strain after some cycles was a result of debonding, which led to the loss of tension stiffening; no practical results showing the strain variation or bond slip between concrete and a steel reinforcing bar were reported. The segmental protection of the strain gauges on the reinforcing bars may have resulted in debonding between concrete and steel reinforcement. However, further investigation is required to observe the bond behavior under fatigue loading of well-anchored embedded reinforcement.

As part of a long-term research program on the improvement of the design and analysis of wind turbine foundations using steel fiber-reinforced concrete, this investigation considers the behavior of shear-critical beams under fatigue loading by observing the principal strain and shear strain evolutions within the planes of the shear spans. Further, the inclination of the principal strains and the bond behavior between concrete and steel reinforcement are considered.

RESEARCH SIGNIFICANCE

This investigation considers the influence of steel fibers in enhancing the fatigue life of shear-critical deep beams. A new approach is presented that shows the comparison between conventional reinforced and steel fiber-reinforced concrete deep beams using progressive average principal and shear strain evolutions within the shear span. Tests have not been previously reported for elements with a shear span to effective depth ratio of less than 2.5. The observed results show that fatigue life of deep beams can be enhanced using steel fibers, and optimized designs of steel fiber fatigue-prone structures can be extended to deep beams.

EXPERIMENTAL PROGRAM

Test specimens

Deep beams with dimensions of 175 x 250 x 700 mm (7 x 10 x 28 in.) were used in this experimental investigation (Fig. 1). The properties of the beams tested are given in

Table 1—Average compressive strength of concrete

Concrete batch	Volume of steel fiber V_f , %	No. of specimens	Average compressive strength f'_c , MPa (ksi)	Standard deviation (compressive strength)	Coefficient of variation (compressive strength)
1	$0V_f^{(*)}$	13	62.6 (9)	6.0	8.5
2	$0V_f^{(†)}$	18	55.1 (8)	2.5	4.6
3	$0.75V_f$	23	55.3 (8)	5.2	9.5
4	$1.5V_f$	24	55.8 (8.1)	5.1	9.1
5	$1.5V_f^{*(‡)}$	8	55.6 (8.1)	2.1	3.7

^(*) $0V_f$ is batch without steel fiber for control beam specimens tested under fatigue loading.

^(†) $0V_f$ is batch without steel fiber for specimens tested under monotonic loading.

^(‡) V_f^* is steel fiber volume for B80-0N1.5 and A97-0F1.5.

Note: V_f is steel fiber volume content (in percentage).

Table 2—Specimen description

Concrete batch	Volume of steel fiber V_f , %	Specimen identification No.	Design f'_c^d , MPa (ksi)	ρ_l , %	ρ_v , %	Maximum fatigue load (% Pu), kN	Minimum fatigue load (% Pu), kN	No. of cycles to failure, N
2	0	C'S	50 (7.3)	0.9	0.2	Monotonic	—	—
2	0	CS	50 (7.3)	0.45	0.2	Monotonic	—	—
1	0	C'-70-0	50 (7.3)	0.9	0.2	70	1.3	210,000
3	0.75	B70-0F0.75	50 (7.3)	0.9	0.2	70	1.3	3,000,000*
4	1.5	B70-0F1.5	50 (7.3)	0.9	0.2	70	1.3	3,000,000*
1	0	C-80-0	50 (7.3)	0.45	0.2	80	1.8	47,000
3	0.75	A80-0F0.75	50 (7.3)	0.45	0.2	80	1.8	66,000
4	1.5	A80-0F1.5	50 (7.3)	0.45	0.2	80	1.8	320,000
5	1.5	A97-0F1.5	50 (7.3)	0.45	0.2	97	1.8	81,000
1	0	C-70-0	50 (7.3)	0.45	0.2	70	1.8	72,000
3	0.75	A70-0F0.75	50 (7.3)	0.45	0.2	70	1.8	123,000
3	0.75	A70-0N0.75	50 (7.3)	0.45	0	70	1.8	260,000
4	1.5	A70-0F1.5	50 (7.3)	0.45	0.2	70	1.8	410,000
1	0	C'-80-0	50 (7.3)	0.9	0.2	80	1.3	62,000
5	1.5	B80-0N1.5	50 (7.3)	0.9	0	80	1.3	650,000

*Specimen did not fail at specified number of cycles.

Notes: V_f is steel fiber volume content (in percentage); f'_c^d is design compressive strength of concrete; ρ_l is longitudinal reinforcement ratio (in percentage); ρ_v is shear reinforcement ratio (in percentage).

Tables 1 and 2. The reinforcement provisions used for the beams surpassed the minimum required in CSA A23.3-04¹⁸ Sections 11.2.8.1 and 11.2.8.2 for shear, 10.5.1.2 for flexure; Eurocode 2-1-1(2004)¹⁹ Section 9.2.2 and 9.2.1.1 for shear and flexure, respectively,¹⁹ and ACI 318-14⁴ Sections R9.6.3.1 and R9.6.1.2 for shear and flexure, respectively.

As a means of ensuring that bond fatigue failure was deliberately averted, adequate anchorage was provided based on code requirements CSA N12.13.1, N12.13.2 (shear reinforcement anchorage), and N12.5.2 (flexural reinforcement anchorage). The bar bending schedule used for anchorage also satisfied EC 2-1-1 (2004) Clause 8.5(1) and (2) for shear reinforcement and 2-1-1 Clause 8.4.1 (1) P for longitudinal reinforcement requirements. The anchorage also satisfied ACI 318⁴ Tables 25.3.1 and 25.3.2 for longitudinal and shear reinforcement, respectively.

Two different steel fiber volume ratios, 0.75% and 1.5%, were examined. High-strength end-hooked steel fibers were used. The geometrical properties of the fibers included

a 30 mm (1.2 in.) fiber length, a diameter of 0.37 mm (0.2 in.), and an aspect ratio of 79. The ultimate tensile stress capacity of the steel fibers was 3070 MPa (445 ksi). Longitudinal reinforcement ratios of 0.45% and 0.90% and shear reinforcement ratios of either 0% or 0.20% were provided in beams having steel fiber volume ratios of 0.75% and 1.50% in this investigation.

In Table 2, the names attached to each beam are given: C'S and CS are assigned to beams (monotonic tests) without steel fibers and reinforced with two 10M and two 15M reinforcing bars, respectively. 15M and 10M reinforcing bars are hot-rolled deformed steel bars with diameters of 16 and 12 mm (0.6 and 0.47 in.), respectively. Similarly, C and C' are assigned to the control beams (beams without steel fibers) reinforced with two 10M and two 15M reinforcing bars, respectively. A and B represent steel fiber-reinforced concrete beams with two 10M and two 15M reinforcing bars. The numbers 70-0, 80-0, 97-0 represent the maximum load level used for the fatigue tests. The letter 'N' denotes

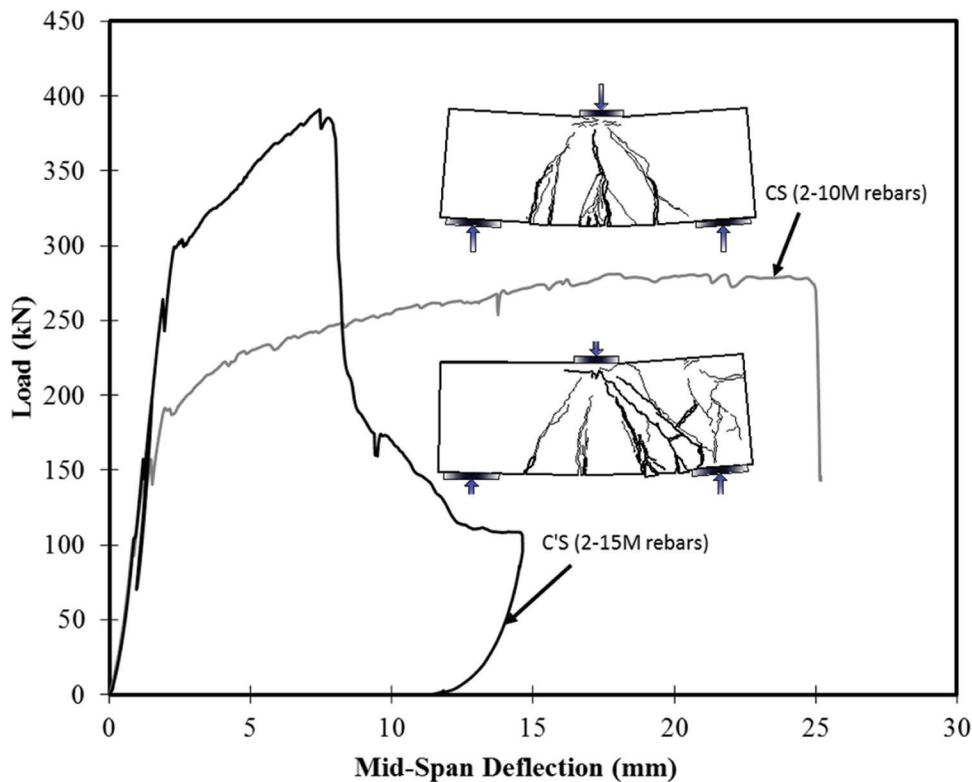


Fig. 2—Load-versus-deflection under monotonic loading (Beams C'S and CS). (Note: 1 kN = 0.225 kip.)

no shear reinforcement, while F0.75 and F1.5 represent the steel fiber volume contents used.

Materials

A design compressive strength of 50 MPa (7 ksi) was selected, with a maximum aggregate size of 10 mm (0.4 in.). The slump readings obtained during concrete casts were between 80 and 150 mm (3 and 6 in.). After casting, the specimens were removed from the curing room at 28 days and placed in a dry compartment. The average compressive strengths of concrete cast for the tests are given in Table 1. The value given in the fourth column of Table 1, for the fatigue loading phase, is equivalent to the average compressive strength within the time frame for testing the beams.

Canadian standard 15M, 10M (deformed steel reinforcing bars), and D4 (cold-worked deformed bar with 5.5 mm [0.22 in.] diameter) bars were used as reinforcement. The D4 reinforcing bars were used for the shear reinforcement. In the beams with shear reinforcement, two 10M reinforcing bars were also provided at the top (hanger bars).

The average yield strength obtained for the 15M, 10M, and D4 reinforcing bars were 430, 480, and 610 MPa (62, 70, and 89 ksi), respectively. The yield strength of the cold-worked steel reinforcing bar corresponded to the 0.2% offset strains. Although the expected yield plateau was absent in cold-worked D4 stress-strain curve, the stresses observed in the shear reinforcement were sufficiently low to justify their use.

Test procedure

Initially two beams, C'S and CS as indicated in Table 2, were tested under monotonic loading. The corresponding failure loads observed were 390 and 270 kN (88 and 61 kip), respec-

tively (Fig. 2). The longitudinal reinforcement ratios were used to observe different failure mechanisms. The failure mode of C'S was observed to be crushing of the compression strut. A combination of shear and flexure was observed in CS, as the fracture of the reinforcing bars occurred at the midspan region. As indicated in the sixth and seventh column of Table 2, percentages of the failure load observed from the monotonic tests were used for the fatigue tests conducted. Each specimen was subjected to fatigue loading without an initial application of monotonic loading.

The fatigue tests were conducted using servo-hydraulic testing equipment having a loading capacity of 350 kN (79 kip). The loading equipment was used to generate a pulsating load of a continuous sinusoidal waveform throughout the test duration. All fatigue tests were conducted at a frequency of 5 Hz, and a constant minimum load of 5 kN (1 kip) was used to prevent backlash due to inertia of the actuator under dynamic loading. The stress ratio resulting from this is considered insignificant.

Instrumentation

Figure 1 shows the details of the beam specimen instrumentation and dimensions. The attached linear variable displacement transducers (LVDTs) were used to measure the evolution of the average strains within the shear span. Using Mohr's circle of strain, the average shear strains, the average principal strains, and the inclination of the principal tensile strain relative to the x- and y-directions within the shear spans of each beam were obtained from strain transformation of the LVDT data (Fig. 3). In Fig. 3, ϵ_2 is the principal tensile strain; ϵ_1 is the principal compressive strain; e_a , e_b , and e_c are the corresponding strains in the directions of the LVDTs; γ_{xy}

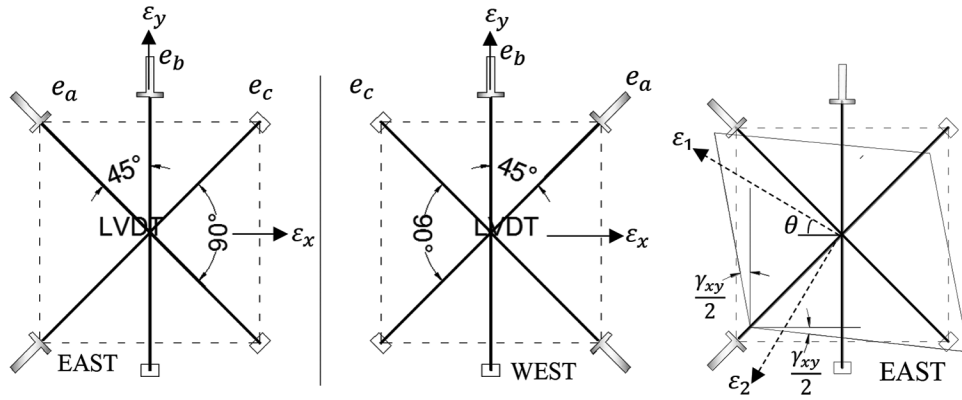


Fig. 3—LVDT strain transformation.

is the average shear strain; ϵ_x and ϵ_y are the average strains in the horizontal and vertical directions, respectively; and θ is the inclination of the average principal tensile strain. A program was developed to generate the deformation evolutions from the laboratory data.

Considering the West LVDTs (γ_{xy} is positive)

$$\epsilon_x = e_c - e_b + e_a$$

where $\epsilon_y = e_b$

$$\gamma_{xy} = e_a - e_c \quad (1)$$

Considering the East LVDTs (γ_{xy} is negative)

$$\epsilon_x = e_c - e_b + e_a$$

where $\epsilon_y = e_b$

$$\gamma_{xy} = e_c - e_a \quad (2)$$

The average principal concrete strains were obtained

$$\epsilon_{1,2} = \frac{1}{2}(\epsilon_x - \epsilon_y) \pm \frac{1}{2} \left(\sqrt{(\epsilon_x - \epsilon_y)^2 + \gamma_{xy}^2} \right) \quad (3)$$

The averages of the strain values obtained from the East and West sets of LVDTs were used. The values for the evolution of θ —the inclination of the principal tensile strain direction—was estimated using γ_{xy} (shear strain), ϵ_x (average strain in the horizontal direction), and ϵ_y (average strain in the vertical direction).

TEST RESULTS AND DISCUSSIONS

The number of cycles leading to failure for each specimen tested under fatigue loading is given in Table 1. The experimental results are expressed in terms of failure modes, principal strain evolutions, shear strain evolutions, midspan deflections, and residual strengths of beams that did not fail after 3,000,000 cycles (Fig. 4 through 16). These are discussed subsequently.

Failure mode

In all beam specimens tested, except Specimens B70-0 F0.75 and B70-0 F1.5 (which sustained 3,000,000 million

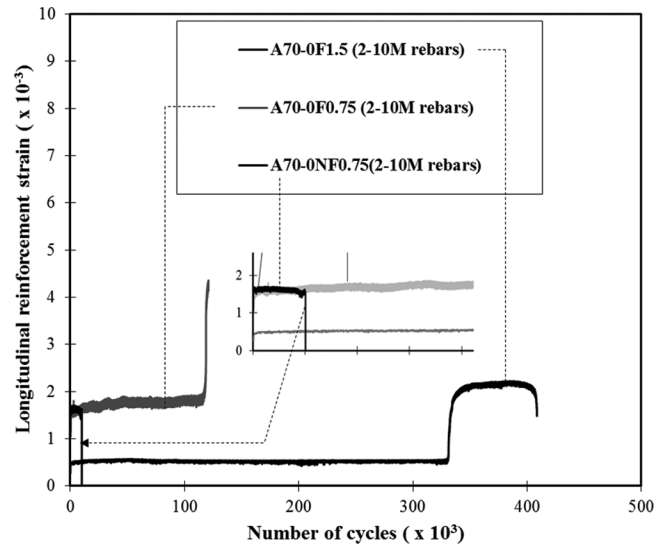


Fig. 4—Longitudinal reinforcement strain versus number of cycles at maximum load (2-10M reinforcing bars).

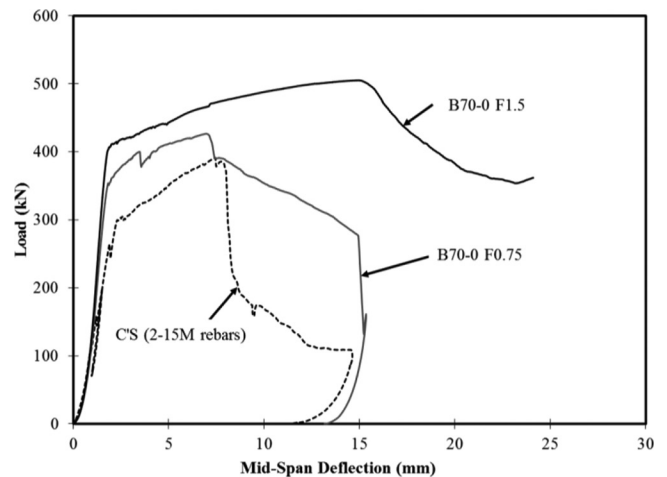


Fig. 5—Load-versus-deformation plot after fatigue loading.

cycles without failure), fracture of the longitudinal reinforcing bars was observed. An increase in fatigue life was observed for the beams as the fiber volume content increased (as shown in Columns 2 and 9 of Table 2). In the steel fiber-reinforced concrete beams, a combination of pullout and fracture of steel fibers was also observed. However, steel fiber pullout was more prevalent, especially in beams reinforced with

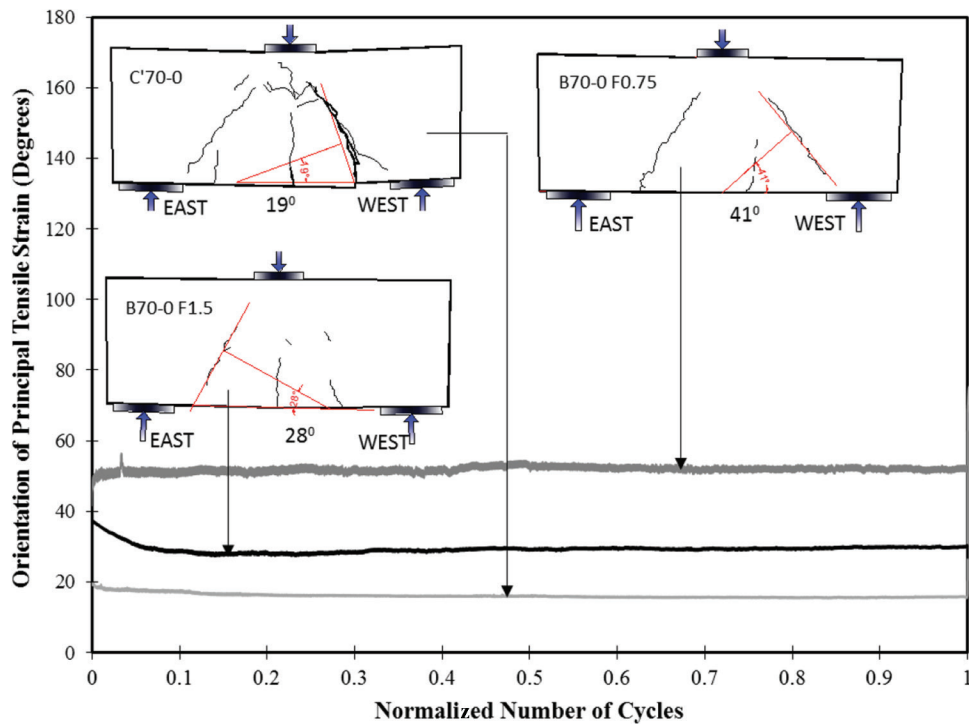


Fig. 6—Crack pattern and inclination of principal tensile strain (15M-70%Pu).

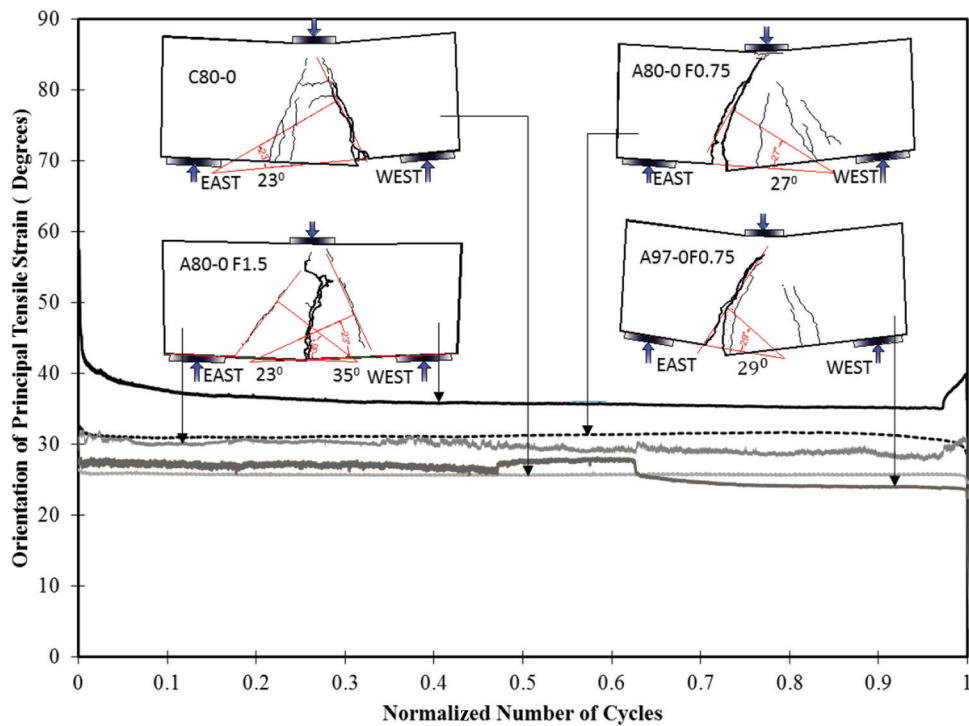


Fig. 7—Crack pattern and inclination of principal tensile strain (10M-80%Pu).

1.5% steel fiber volume ratio compared to beams with 0.75% steel fiber volume ratio. This is attributed to lower stresses induced in steel fibers with 1.5% steel fiber volume ratio at crack bridges; hence, bond resistance between steel fibers and concrete governed. On the other hand, fracture of steel fiber predominates due to high stresses. Throughout the tests conducted, no fracture of shear reinforcement was observed. This observation is consistent with those reported

in the literature for conventional reinforced concrete deep beams.^{1,2}

The strain induced in the longitudinal reinforcing bars was observed to reduce as the steel fiber volume ratio increased from 0.75% to 1.5%. (for example, refer to Fig. 4 for beams with two 10M reinforcing bars). The strain evolution for Beam A70-0NF0.75 reinforced with two 10M reinforcing bars was truncated after 10,000 cycles due to a malfunction of the strain gauge attached to the longitudinal reinforce-

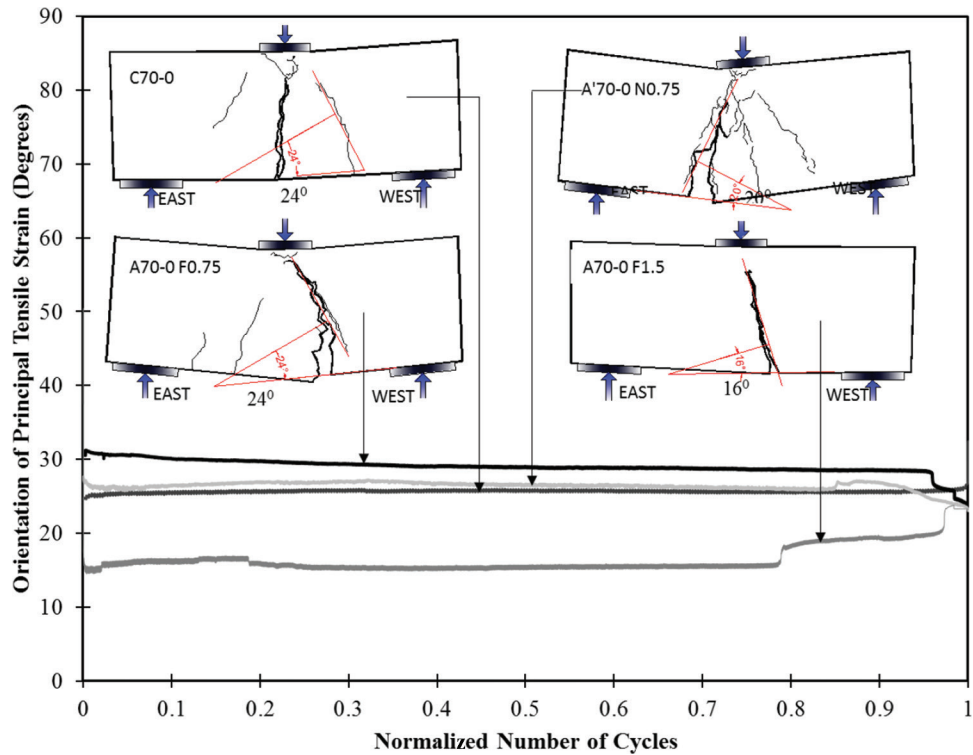


Fig. 8—Crack pattern and inclination of principal tensile strain (10M-70%Pu).

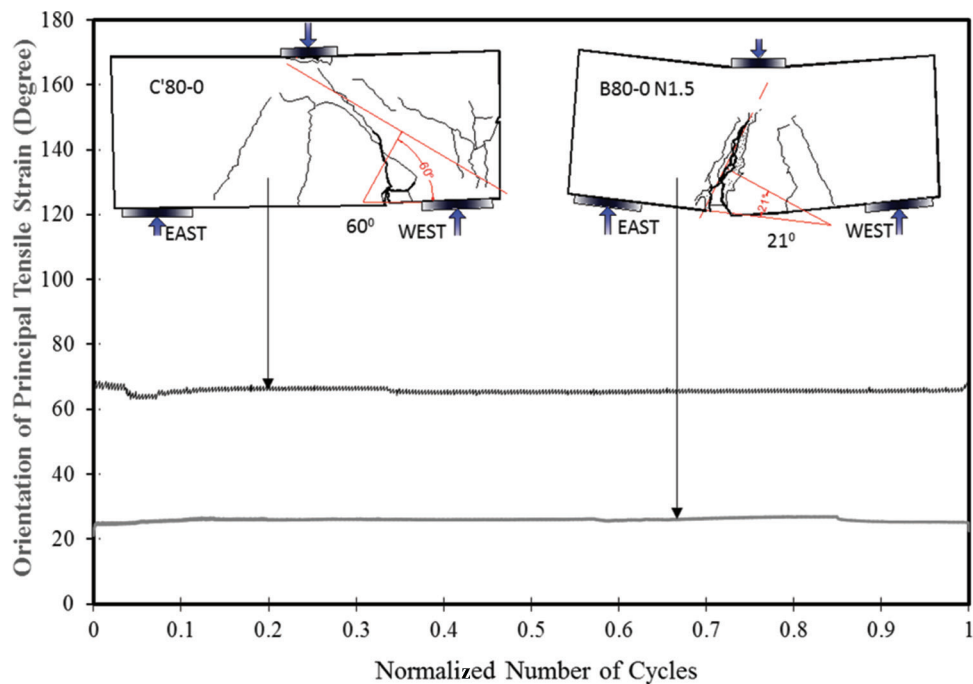


Fig. 9—Crack pattern and inclination of principal tensile strain (15M-80%Pu).

ment. The reinforcement strain evolutions shown in Fig. 4 were obtained from the region at which fracture occurred, hence, close to the maximum strain along the longitudinal reinforcement. As also reported in the literature on flexural beams,^{16,17} the reduced strain or stress values (attributed to the addition of steel fibers) resulted in the enhanced fatigue life of the steel fiber-reinforced concrete beams.

As shown in the deformation evolution plots (Fig. 10 to 15) for conventional and steel fiber-reinforced concrete

beams, after significant fracture of the longitudinal reinforcement, sudden collapse of steel fiber-reinforced concrete beams did not occur immediately thereafter. The presence of steel fibers resulted in the beams resisting more cycles under high deformation before final fracture. This is attributed to crack-bridging of steel fibers.

Because Specimens B70-0 F0.75 and B70-0 F1.5 did not fail after 3,000,000 cycles, the beams were further subjected to monotonic loading (Fig. 5). The observed residual

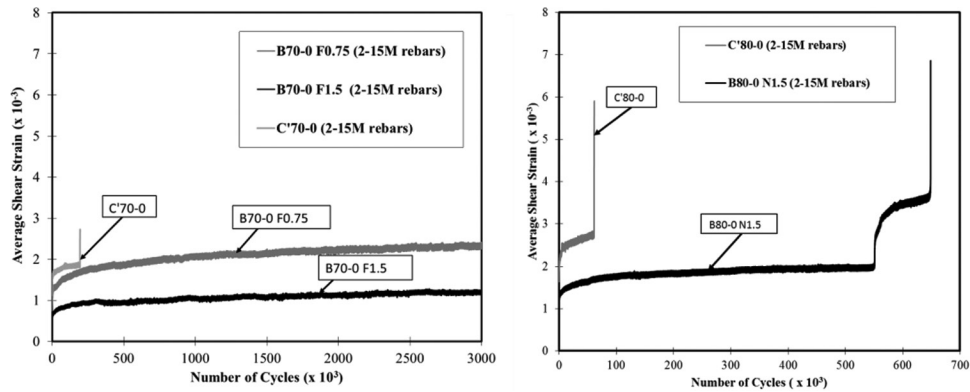


Fig. 10—Average shear strain evolution (2-15M).

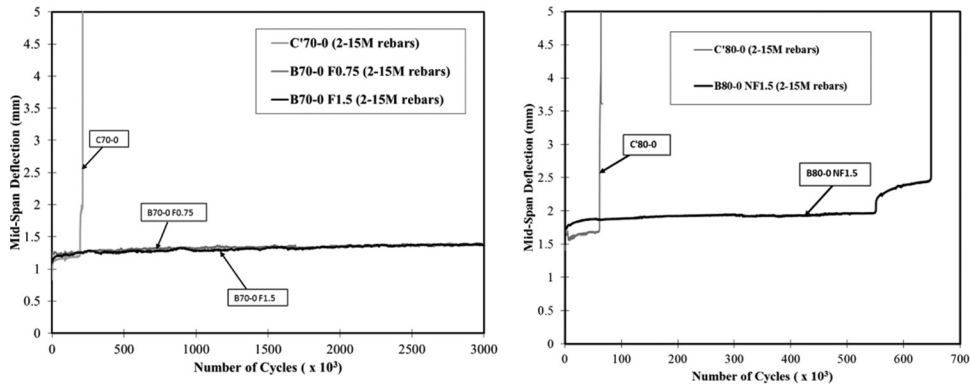


Fig. 11—Midspan deflection (2-15M).

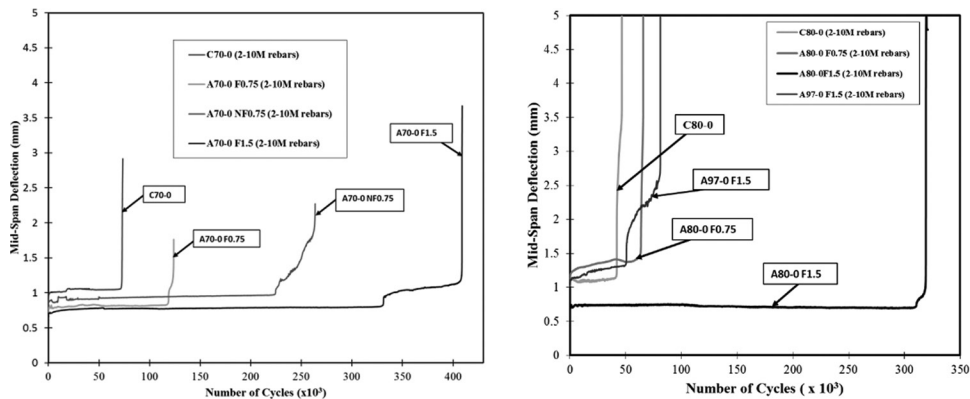


Fig. 12—Midspan deflection (2-10M).

strength for the two beams were higher than the capacity of the conventional reinforced concrete beam without fatigue damage. This further shows that reduced section sizes obtainable in steel fiber-reinforced concrete beams can be used to achieve the same fatigue life as in larger conventional reinforced concrete beams.

Crack pattern

During fatigue loading, flexural and shear-flexural cracks were initially observed on the surfaces of the beams reinforced with two 10M reinforcing bars (under-reinforced beams). Inclined and diagonal cracks accompanied such cracks in a few of the two 10M reinforced beams and in beams reinforced with two 15M reinforcing bars. Final fatigue failure observed in each specimen occurred at

a major crack plane that developed from the onset of the fatigue tests. The failure regions are shown in Fig. 6 to 9 with thick crack patterns.

After fracture of the longitudinal reinforcement, sudden collapse of the steel fiber-reinforced concrete beams did not occur immediately thereafter. The presence of steel fibers resulted in the beams resisting more cycles under high deformation before final fracture.

Specimen A70-0NF0.75 failed after approximately 260,000 cycles (more than twice the number of cycles to failure for Specimen A70-0F0.75 with shear reinforcement). As observed in Fig. 4, the two specimens started approximately at similar strain values. The increase in fatigue life of the specimen without shear reinforcement may be attributed to stress redistribution (leading to reduced strain in the rein-

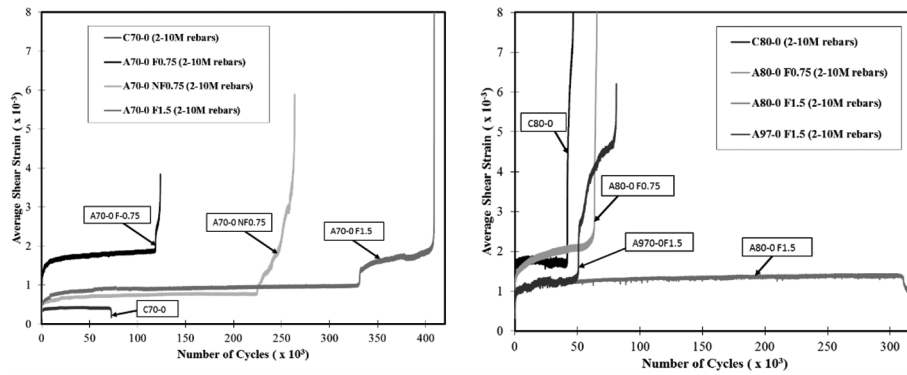


Fig. 13—Average shear strain evolution (2-10M).

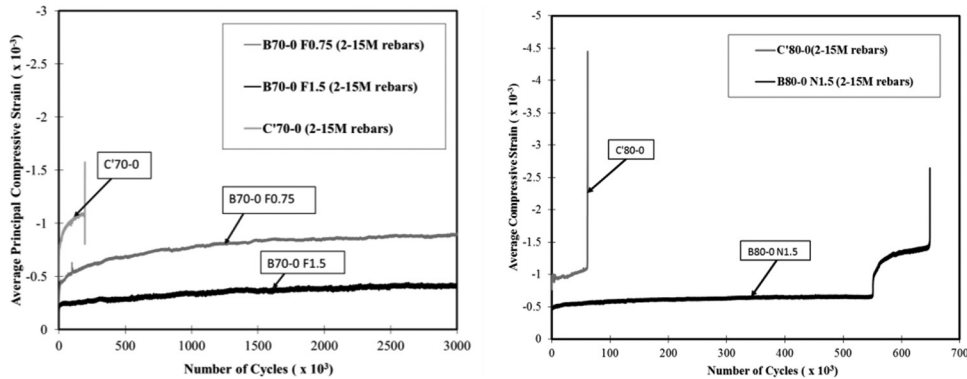


Fig. 14—Average principal compressive strain evolution (2-15M).

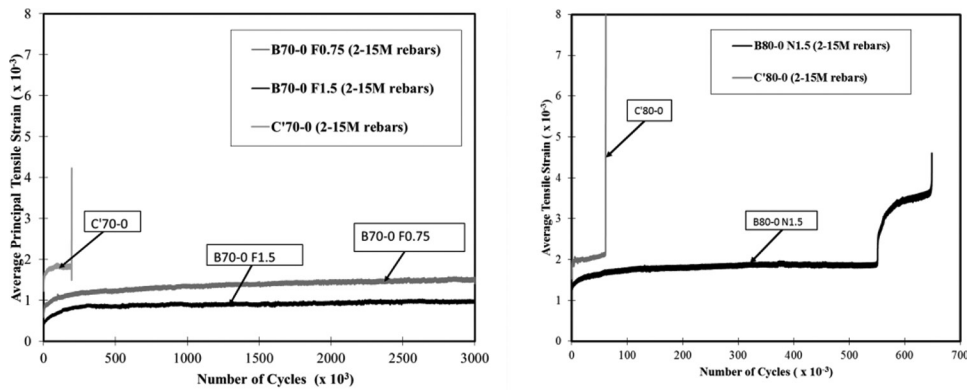


Fig. 15—Average principal tensile strain evolution (2-15M).

forcement) as a result of more fatigue cracks on the surface of Specimen A70-0NF0.75. As such, active bridging contribution of the fibers intersecting the cracks occurred (Fig. 8).

The approximate orientations of the fatigue failure planes were estimated from strain transformations of the LVDT data obtained from the experiments. The obtained evolutions further show that the accuracy of instrumentation used was acceptable. From Fig. 6 to 9, no significant change in the orientation of the principal strain evolution was observed except at the initial stage of loading, at the point of reinforcement fracture, and at failure.

Shear strain evolution/midspan deflection

Under fatigue loading of the shear-critical beams (Specimen C'S), shear forces are transferred through the compression struts to the supports, and irreversible compressive

strain accumulates due to the induced compressive stress within the shear span. To maintain equilibrium, the horizontal tensile forces are resisted by the longitudinal reinforcement.

With the addition of steel fibers to the beams reinforced with two 15M reinforcing bars, the shear span deformations (shear strains) were observed to reduce as the steel fiber volume ratio increased from 0% to 1.5% (refer to Fig. 10). Additionally, insignificant increases in the midspan deflections were observed (Fig. 11). This improvement was as a result of crack-bridging of the inclined cracks within the shear span, hence, retarding the shear strains. However, the obvious increase in the deflection evolution of Specimen B80-0NF1.5 was also attributed to the fact that there was no shear reinforcement and no top reinforcing bars (hanger bars).

After fatigue cracks at the midspan occurred in the conventional under-reinforced concrete deep beams with two

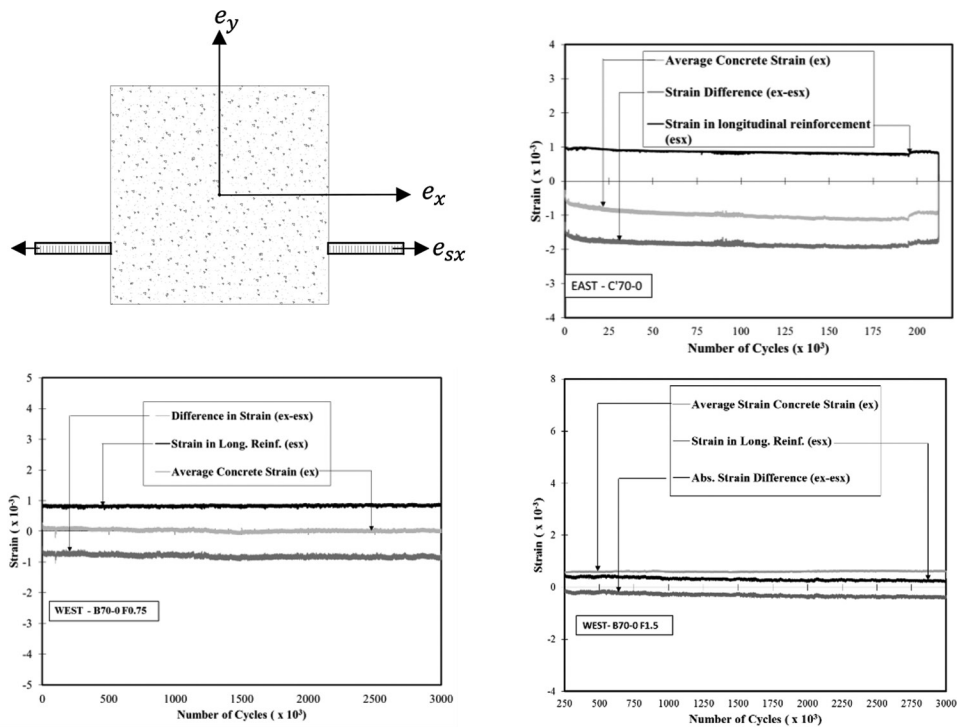


Fig. 16—Evolution of concrete and reinforcement strain variation.

10M reinforcing bars (Specimen CS), the aforementioned mechanism in which shear force is transferred through the compression strut to the support under fatigue loading no longer holds. This is attributed to the fact that the beams are subsequently governed by the reinforcement crack propagation at the intersection with the midspan cracks, resulting in increased rotation.

Beams governed by flexure (beams reinforced with two 10M reinforcing bars) were observed to exhibit reduced midspan deflections under fatigue loading as the steel fiber volume ratio increased from 0% to 1.5% (refer to Fig. 12). On the other hand, the shear span deformation (shear strain evolution) also increased, corresponding to an increase in the capacity for shear force transfer through concrete struts (refer to Fig. 13).

Under high fatigue loads (80% of static capacity of CS beam), a steel fiber volume ratio of 1.5% reduced both the midspan deflection and shear span deformation of Beam A80-0F1.5 compared to Beams A80-0F0.75 and C80-0 (Fig. 12 and 13). Although the use of 0.75% steel fiber volume ratio enhanced the fatigue life, it was ineffective in reducing the shear span deformation and midspan deflection under high fatigue loading when compared with the Control Beam C80-0. This was attributed to early pullout and fracture of the steel fibers under high loads.

At a fatigue loading of 97% of the static capacity of the CS beam, the fatigue life of A97-0F1.5 was observed to be higher than the fatigue life obtained using 0.75% steel fiber volume ratio and fatigue loading of 80% of the static capacity of Beam CS. In addition, the shear span deformation and midspan deflection were observed to be lower when compared to those of Beams A80-0F0.75 and C80-0. More steel fibers at the intersection with the concrete crack in Beam A97-0F1.5 resulted in lower induced bond stresses between

fibers and concrete, and lower induced stresses in the fibers when compared with Beams A80-0F0.75 and C80-0. These results further demonstrate the enhancing influence of steel fiber volume ratio of 1.5% under high fatigue loading.

Average principal strain evolution

As previously indicated, various tests have been conducted to observe the fatigue resistance properties of steel fiber-reinforced concrete. However, most tests have been conducted on specimens in flexure and compression. Although tests in flexure indicated fatigue life enhancement with steel fibers, there have been conflicting observations on the behavior in compression.⁶ Considering the beams governed by crushing of concrete under static loading (using specimens reinforced with two 15M reinforcing bars), the observed strain transformations of LVDT data show substantial reduction in the values of the average compressive and tensile strain evolutions under fatigue loading as the steel fiber volume ratio increased from 0% to 1.5% (refer to Fig. 14 and 15). On the other hand, the increase in the tensile and compressive strain evolutions in beams reinforced with two 10M reinforcing bars indicate that more stresses are transferred to the support through the compressive strut, since lower deflections were observed.

Bond behavior

In the literature, investigations conducted on the influence of bond deterioration under fatigue loading were based on beams with non-anchored reinforcing bars. Such specimens were deliberately allowed to fail by bond slip under fatigue loading.²⁰ However, the beams tested in this investigation were provided with adequate anchorage based on code provisions.

Under fatigue loading, provided one of the followings is observed, severe damage to the bond between concrete and steel reinforcement will not occur (Fig. 16): 1) the evolutions of the concrete and reinforcement strains (both in the direction of the reinforcement) are approximately parallel; and 2) the evolution of the difference between the concrete strain evolution and reinforcement strain evolution is approximately constant.

The average strain evolution of concrete in the horizontal direction and the strain gauge reading on the longitudinal reinforcing bars were obtained for the beams tested. Obtaining full evolution readings was not successful for all the beams because some connections of the strain gauges malfunctioned when intersected by concrete cracks. However, results obtained from beams tested (with two 15M reinforcing bars) at 70% of the static capacity are presented in Fig. 16. From this figure, reasonable integrity of bond between concrete and steel reinforcement within the shear span can be inferred; however, the use of high-strength concrete also contributed to the bond integrity.

COST-EFFECTIVENESS OF STEEL FIBERS

Although it has been shown that steel fibers enhance the fatigue life of concrete deep beams, a reasonable comparison in terms of cost between conventional reinforced concrete and steel fiber-reinforced concrete is necessary. Only then can the effective cost reduction derived from the use of steel fiber-reinforced concrete be ascertained.

Because Beams B70-0F0.75 and B70-0F1.5 sustained 3,000,000 cycles without failing, the corresponding size of a conventional reinforced concrete beam that will achieve at least 3,000,000 cycles was obtained using typical design procedures.

Table 3—Cost comparison between plain and fiber-reinforced concrete

Materials	Quantity	Unit	Cost (\$)	Quantity	Unit	Cost (\$)
Coarse aggregate	32	kg	1.0	240	kg	7.0
Fine aggregate	26	kg	0.7	195	kg	4.9
Cement	14	kg	3.4	109	kg	26.5
Labor cost	402	ft ²	442	1065	ft ²	1171
Steel fiber	3.5	kg	4.2			
Total	B70-0F1.5		451	Equivalent beam		1209

The stress induced in steel reinforcement that will cause fatigue failure after 3,000,000 cycles was initially estimated using a method described in the literature.^{3,21,22} By keeping the shear span to effective depth ratio and reinforcement ratios constant, a strut-and-tie analysis approach was used to obtain the size of a conventional reinforced concrete deep beam with a fatigue life of 3,000,000 cycles.^{3,23}

In Table 3, the difference in cost of required conventional reinforced concrete and steel fiber-reinforced concrete are given. The costs were based on coarse aggregate (\$27.5/ton USD), fine aggregates (\$25/ton USD), cement (\$10.47/ton USD), labor cost of reinforcement installation (\$1.1/ft² USD), and steel fibers (\$1200/ton USD). The increase in reinforcement lengths and amount, extra costs for formwork, and water required in the equivalent beam without steel fibers were excluded (Fig. 17).

From the total cost, it is seen that the cost of the conventional reinforced concrete section that will sustain 3,000,000 cycles is approximately three times the cost of steel fiber-reinforced concrete section.

CONCLUSIONS

The influence of steel fibers in enhancing the fatigue life of deep beams was investigated by comparing conventional reinforced concrete deep beams with steel fiber-reinforced concrete deep beams. Shear reinforcement ratio, steel-fiber volume ratio, and longitudinal reinforcement ratio were varied. A new approach was used to estimating the deformation evolution within the shear spans of each beam tested. Based on the results of the test program, the following conclusions are drawn:

1. Deep beams with shear span to effective depth ratio below 1.5 (1.25 was used for this investigation) may fail by the fracture of longitudinal reinforcement rather than shear reinforcement. This is attributed to the low amount of stresses induced in the shear reinforcement. These observations have also been previously reported in the literature for deep beams.
2. The fatigue life of reinforced concrete deep beams with shear reinforcement can be enhanced using steel fibers. In addition, depending on the reinforcement ratio, the corresponding deformations are reduced with the inclusion of steel fibers.
3. The use of steel fibers proved to be effective in enhancing fatigue life and reducing the deformation of beams without

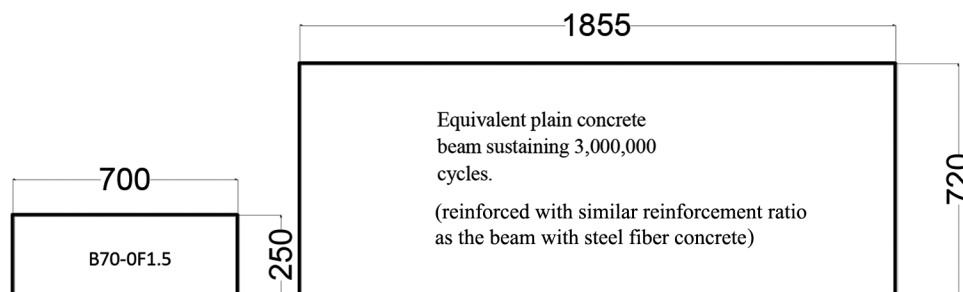


Fig. 17—Comparison between steel fiber-reinforced beam and conventional reinforced concrete beam. (Note: Dimensions are in mm; 1 mm = 0.0394 in.)

shear reinforcement. However, it is recommended that larger beams be tested to confirm this observation.

4. Based on the observed results of the experiments conducted, the design of fatigue-critical structures can be optimized with reduced section sizes using steel fiber-reinforced concrete. The beneficial effect will be more substantial (in terms of cost) in very large structures that are designed with reduced volumes of steel fiber concrete.

AUTHOR BIOS

Benard Isojeh is a PhD Candidate in civil engineering at the University of Toronto, Toronto, ON, Canada. His research interests include improvement in the design and analysis of wind turbine foundations with a focus on fatigue analysis.

Maria El-Zeghayar is a Civil Engineer in the Renewable Power Business Unit at Hatch Ltd. She received her PhD from the University of Waterloo, Waterloo, ON, Canada, in 2011. Her research interests include fatigue analysis of materials.

Frank J. Vecchio, F.A.C.I., is a Professor and Bahen/Tanenbaum Chair in civil engineering at the University of Toronto. He is a member of Joint ACI-ASCE Committees 441, Reinforced Concrete Columns, and 447, Finite Element Analysis of Reinforced Concrete Structures. He received the 1998 ACI Structural Research Award, the 1999 ACI Structural Engineer Award, the 2011 ACI Wason Medal, and the 2016 Joe Kelley Award. His research interests include improved analysis and design of reinforced concrete structures, development of nonlinear analysis procedures, development of constitutive models, analysis of repaired and rehabilitated structures, and forensic assessment of distressed or failed structures.

ACKNOWLEDGMENTS

The authors gratefully acknowledge the Natural Science and Engineering Research Council (NSERC) of Canada and Hatch Ltd for the invaluable contributions and financial support to this research. The authors also acknowledge the assistance received from the Niger Delta Development Commission and the Delta State Government of Nigeria for the duration of this research.

REFERENCES

1. Teng, S.; Ma, W.; Tan, K. H.; and Kong, F. K., "Fatigue Tests of Reinforced Concrete Deep Beams," *The Structural Engineer*, V. 76, No. 18, 1998, pp. 347-352.
2. Teng, S.; Ma, W.; Tan, K. H.; and Wang, F., "Shear Strength of Concrete Deep Beams under Fatigue Loading," *ACI Structural Journal*, V. 95, No. 4, July-Aug. 2000, pp. 572-580.
3. Isojeh, M. B., and Vecchio, F. J., "Parametric Damage of Concrete under High-Cycle Fatigue Loading in Compression," 9th International Conference on Fracture Mechanics of Concrete and Concrete Structures (FraMCoS-9), 2016, 12 pp..
4. ACI 318-14 to ACI 346-09, *Manual of Concrete Practice: Part 3*, American Concrete Institute, Farmington Hills, MI, 2015.
5. Huang, C., and Zhao, G., "Properties of Steel Fiber Reinforced Concrete Containing Larger Coarse Aggregate," *Cement and Concrete Composites*, V. 17, No. 3, 1995, pp. 199-206. doi: 10.1016/0958-9465(95)00012-2
6. Naaman, A. E., and Reinhardt, H. W., eds., *High Performance Fiber Reinforced Cement Composites 2 (HPFRCC2)*, Proceedings of the Second International RILEM Workshop, 1996, 502 pp.
7. Lee, M. K., and Barr, B. I. G., "An Overview of the Fatigue Behavior of Plain and Fiber Reinforced Concrete," *Cement and Concrete Composites*, V. 26, No. 4, 2004, pp. 299-305. doi: 10.1016/S0958-9465(02)00139-7
8. ACI Committee 544, "Design Considerations for Steel Fiber Reinforced Concrete (ACI 544.4R-88) (Reapproved 1999)," American Concrete Institute, Farmington Hills, MI, 1999, 18 pp.
9. ACI Committee 544, "State-of-the-Art Report on Fiber Reinforced Concrete (ACI 544.1R-82)," American Concrete Institute, Farmington Hills, MI, 1982, 22 pp.
10. Ramakrishnan, V.; Wu, Y. G.; and Hossali, G., "Flexural Fatigue Strength, Endurance Limit and Impact Strength of Fiber Reinforced Concretes," Transportation Research Board, Washington, DC, 1989, pp. 17-24.
11. Nanni, A., "Fatigue Behavior of Steel Fiber Reinforced Concrete," *Cement and Concrete Composites*, V. 13, No. 4, 1991, pp. 239-245. doi: 10.1016/0958-9465(91)90029-H
12. Chang, D., and Chai, W., "Flexural Fracture and Fatigue Behavior of Steel Fiber-Reinforced Concrete Structures," *Nuclear Engineering and Design*, V. 156, No. 1-2, 1995, pp. 201-207. doi: 10.1016/0029-5493(94)00946-V
13. Naaman, A. E., and Hammoud, H., "Fatigue Characteristics of High Performance Fiber-Reinforced Concrete," *Cement and Concrete Composites*, V. 20, No. 5, 1998, pp. 353-363. doi: 10.1016/S0958-9465(98)00004-3
14. Komeling, H. A.; Reinhardt, H. W.; and Shah, S. P., "Static and Fatigue Properties of Concrete Beams Reinforced with Continuous Bar and with Fibers," *ACI Journal Proceedings*, V. 77, No. 1, Jan.-Feb. 1980, pp. 36-43.
15. Kwak, K.; Suh, J.; and Hsu, T., "Shear-Fatigue Behavior of Steel Fiber Reinforced Concrete Beams," *ACI Structural Journal*, V. 88, No. 2, Mar.-Apr. 1991, pp. 155-160.
16. Parvez, A., and Foster, S. J., "Fatigue Behavior of Reinforced Concrete Beams with Addition of Steel Fibers," *From Materials to Structures: Advancement through Innovation-Samali*, Attard and Song, eds., 2013.
17. Parvez, A., and Foster, S. J., "Fatigue Behavior of Steel-Fiber-Reinforced Concrete Beams," *Journal of Structural Engineering*, ASCE, V. 141, No. 4, 2015, p. 04014117 doi: 10.1061/(ASCE)ST.1943-541X.0001074
18. CSA (Canadian Standards Association), "Design of Concrete Structures (CSA A23.3)," Mississauga, ON, Canada, 2004, 232 pp.
19. Eurocode 2 (EC2), "Design of Concrete Structures – Part 1-1: General Rules for Buildings (BS EN 1992-1-1)," British Standards Institution, London, UK, 2004, 225 pp.
20. Hawkins, N. M., "Fatigue Characteristics in Bond and Shear of Reinforced Concrete Beams," *Fatigue of Concrete*, SP-41, American Concrete Institute, Farmington Hills, MI, 1974, pp. 203-236.
21. Goransson, F., and Nordenmark, A., "Fatigue Assessment of Concrete Foundations for Wind Power Plants," master's thesis, Department of Civil and Environmental Engineering, Chalmers University of Technology, Goteborg, Sweden, 2011, 74 pp..
22. Rocha, M., and Bruhwiler, E., "Prediction of Fatigue Life of Reinforced Concrete Bridges," *Bridge Maintenance, Safety, Management, Resilience and Sustainability*, Biondini and Frangopol, eds., pp. 3755-3760.
23. Herwig, A., "Reinforced Concrete Bridges under Increased Railway Traffic Loads—Fatigue Behavior and Safety Measures," PhD thesis No. 4010, Ecole Polytechnique Federale de Lausanne, Lausanne, Switzerland, 2008, 142 pp.